Physical Chemistry Chemical Physics

Dynamic Article Links ►

Supporting Information

Cite this: DOI: 10.1039/c0xx00000x

www.rsc.org/xxxxxx

Evanescent Photosynthesis: Exciting cyanobacteria in a surface-confined light field

Matthew D. Ooms[a], Vincent J. Sieben[a], Scott C. Pierobon[a], Erica E. Jung[b], Michael Kalontarov[b], David Erickson[b] and David Sinton*[a]

Received (in XXX, XXX) Xth XXXXXXXXX 20XX, Accepted Xth XXXXXXXXX 20XX
DOI: 10.1039/b000000x

[a] Department of Mechanical and Industrial Engineering, University of Toronto, Toronto, ON, Canada, M5S 1A1. Fax: 1-416-978-7753; Tel: 1- 416-978-1623; E-mail: sinton@mie.utoronto.ca
[b] Sibley School of Mechanical and Aerospace Engineering, Cornell University, Ithaca, NY, USA, 14853. Fax: 1-607-255-1222; Tel: 1-607-255-4861; E-mail: de54@cornell.edu.

Model Details

A un-polarized Helium-Neon laser with a circular cross-section beam profile can be modelled as a Gaussian using the following equation (TEM00) [1]:

$$I_{n1}(r,a) = I_0(a)\, e^{-2(r^2)/w(a)^2} \qquad (1)$$

where r is the radius from the beam center, a is the distance from the beam waist, $w(a)$ is the beam width and $I_0(a)$ is the peak intensity, both at distance a. After determining the intensity profile for the apparatus shown in Fig. 1 of the paper at the air-to-prism interface (n_1 to n_2 - before the beam enters the prism), the Fresnel transmission coefficients for both s- and p-polarizations (t_1^s and t_1^p, respectively) were used to determine the intensity profile of the beam in the prism:

$$I_{0,n2} = \begin{cases} |t_1^s|^2 \cdot I_{0,n1}, & s-\text{pol} \\ |t_1^p|^2 \cdot I_{0,n1}, & p-\text{pol} \end{cases} \qquad (2)$$

$$t_1^s = \frac{2n_1 \cos\theta_{i1}}{n_1\cos\theta_{i1} + n_2\cos\theta_{t1}} \qquad (3)$$

$$t_1^p = \frac{2n_1 \cos\theta_{i1}}{n_1\cos\theta_{t1} + n_2\cos\theta_{i1}} \qquad (4)$$

where, θ_{i1} is the incident angle ($\theta_{i1} = 45^o - \theta_{laser}$) and θ_{t1} is the transmitted angle (calculated from Snell's law) at the air-prism interface. The evanescent intensity profile at the prism-sample interface was calculated for s-polarized and p-polarized light using the matrix formalization as described in references [2-6]. The matrix method is useful because it can be used to account for multi-layered systems (i.e. index matching fluid, different slide and prism materials, etc.) [4, 7]. The formulae for this method are:

$$I_{0,n3} = \begin{cases} |t_2^s|^2 \cdot I_{0,n2}, & s-\text{pol} \\ C_p \cdot |t_2^p|^2 \cdot I_{0,n2}, & p-\text{pol} \end{cases} \qquad (5)$$

$$\text{where } t_2^{s,p} = \frac{1}{M_{11}^{s,p}} \text{ and } C_p = |\cos\theta_{ts}|^2 + |\sin\theta_{ts}|^2 \qquad (6)$$

$$\textit{and } \begin{pmatrix} E_i \\ E_r \end{pmatrix} = M^{s,p} \begin{pmatrix} E_t \\ 0 \end{pmatrix} \qquad (7)$$

where $M^{s,p}$ is the matrix of the stack that links the incident, reflected and transmitted electric fields (E_i, E_r, E_t) for s- or p-polarised light, C_p is the magnitude factor that takes into account the two field components of p-polarised light for total internal reflection as in Axelrod et al. [5, 6] and θ_{ts} is the final transmitted angle (imaginary, calculated from Snell's law) at the sample interface. The overall matrix can be calculated for N layers (l = 0, 1, 2, ..., s) from the dynamical and the propagation matrices (D_l and P_l) as:

$$M^{s,p} = \begin{pmatrix} M_{11} & M_{12} \\ M_{21} & M_{22} \end{pmatrix} = D_0^{-1}\left[\prod_{l=1}^{N} D_l P_l D_l^{-1}\right] D_s \qquad (8)$$

$$D_l = \begin{cases} \begin{pmatrix} 1 & 1 \\ n_l\cos\theta_l & -n_l\cos\theta_l \end{pmatrix}, & \text{for s} - \text{pol} \\ \begin{pmatrix} \cos\theta_l & \cos\theta_l \\ n_l & -n_l \end{pmatrix}, & \text{for p} - \text{pol} \end{cases} \qquad (9)$$

$$P_l = \begin{pmatrix} e^{-ik_l d_l} & 0 \\ 0 & e^{ik_l d_l} \end{pmatrix}, \text{ where } k_l = n_l \frac{w}{c}\cos\theta_l \qquad (10)$$

where for each layer: n_l is the complex index of refraction, θ_l is the complex angle of propagation (to the normal, determined by Snell's law), k_l is the component of the wave vector along the direction of propagation, d_l is the thickness of the thin film and w is the angular frequency of light. The evanescent intensity at any position perpendicular to the TIR interface decays exponentially with z as [5]:

$$I_{n3}(z) = I_{0,n3}\, e^{-z/d} \quad (11)$$

$$\text{where, } d_{pen} = \frac{\lambda_0}{4\pi}[n_1^2 \sin^2\theta_{i2} - n_3^2]^{-1/2} \quad (12)$$

where λ_0 is the light wavelength in vacuum, $\theta_{i2} = 45^o + \theta_{t1}$ is the incident angle with reference to the top of the prism and n_3 is the index of refraction in the liquid sample. In this work the model was applied to the two-layer system of glass and media.

The evanescent intensity amplitudes were spatially mapped from the initial laser-profile (circular) to the prism-sample interface (elliptical). Since the interface surfaces are normal to the plane of incidence, the spatial profile will be distorted only in one dimension, calculated using the cosine of the incident angle.

Supplemental Experimental Results

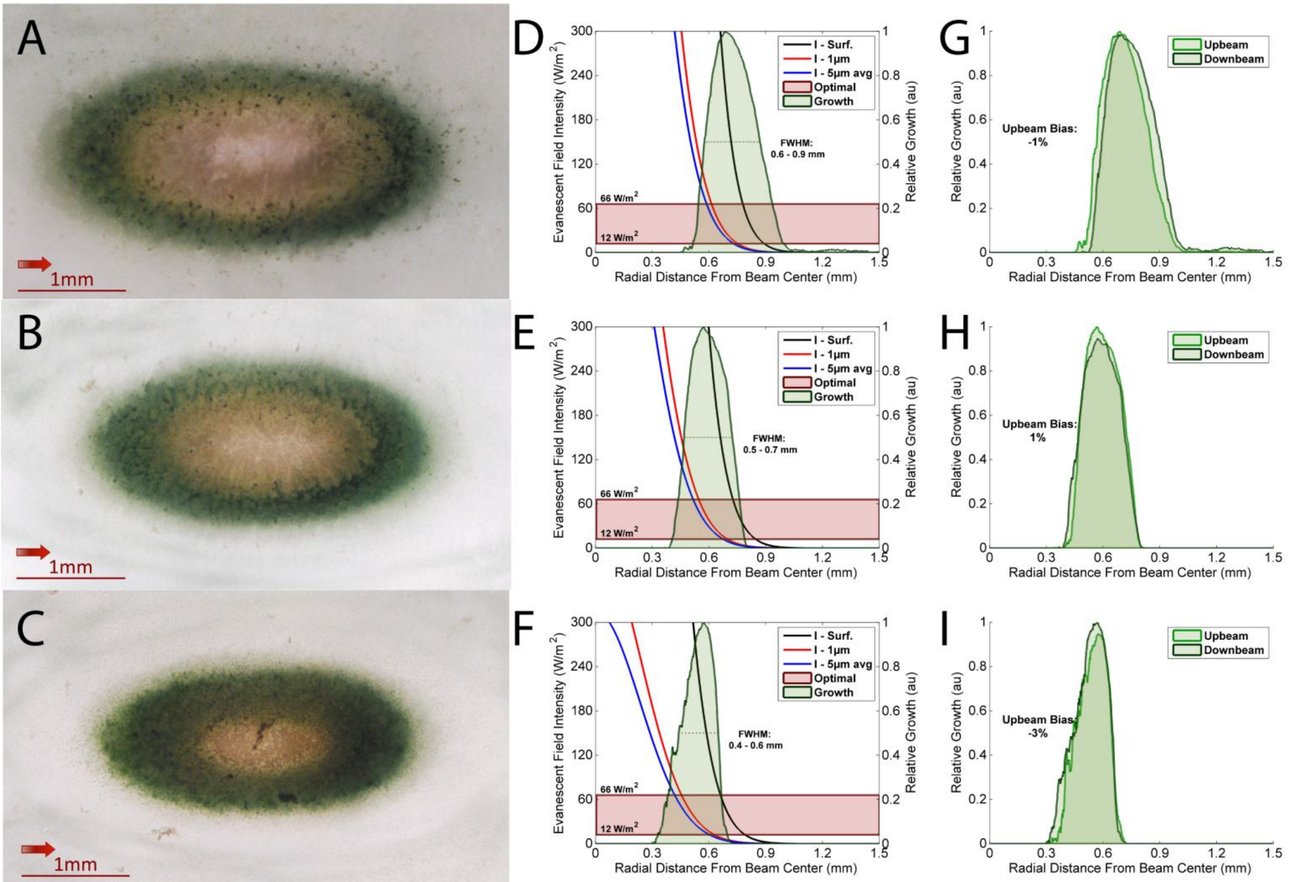

Fig. S1 Results from secondary evanescent light based growth experiments collected using the methods described in the paper. (A-C) Images of cyanobacteria growth patterns resulting from evanescent excitation at the glass-media interface for incident light powers of 1mW, 0.5mW, and 0.25mW, respectively. The elliptical growth patterns correspond to the evanescent field geometry, and shows distinct regions of photoinhibition (centre), and growth, surrounded by negligible growth. (D-F) Corresponding growth profiles for each light power with the corresponding evanescent field intensities plotted at the surface, 1 μm above the surface, and as a 5-μm average. The power range determined from the direct radiation experiments (Fig. 2) is shown by the red band for reference. (G-I) Quantification of the upbeam/downbeam growth bias for each respective ring pattern indicating the relative degree of growth intensity relative to the center of the beam profile in either the left (downbeam) or right (upbeam) direction.

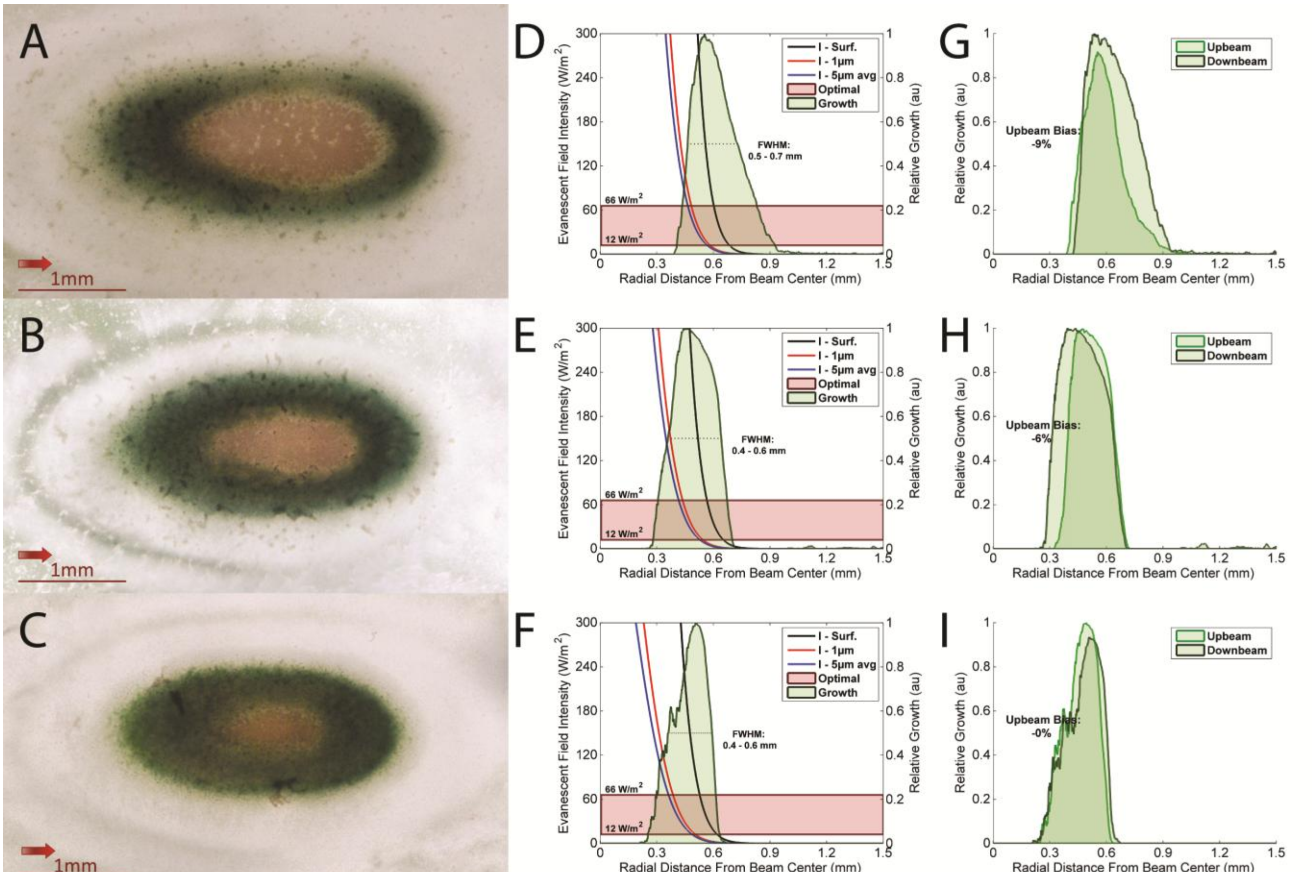

Fig. S2 Results from tertiary evanescent light based growth experiments collected using the methods described in the paper, and plotted as in Fig. S1. (A-C) Images of cyanobacteria growth patterns resulting from evanescent excitation at the glass-media interface for incident light powers of 1mW, 0.5mW, and 0. 25mW, respectively. (D-F) Corresponding growth profiles for each light power with the corresponding evanescent field intensities plotted at the surface, 1 µm above the surface, and as a 5-µm average. (G-I) Quantification of the upbeam/downbeam growth bias for each respective ring pattern indicating the relative degree of growth intensity relative to the center of the beam profile in either the left (downbeam) or right (upbeam) direction.

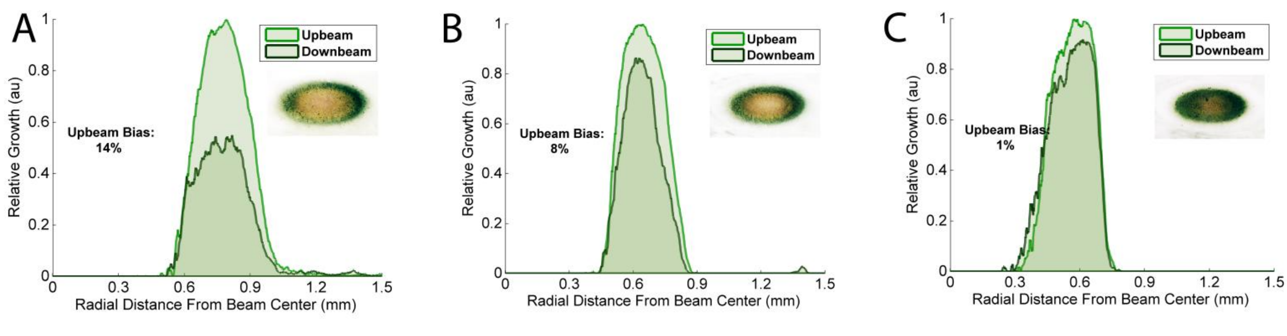

Fig. S3 Quantification of the upbeam/downbeam growth bias for the growth patterns presented in Fig 5*A-C* indicating the degree of growth intensity relative to the center of the beam profile in either the left (downbeam) or right (upbeam) direction. Graphs correspond to laser powers of (A) 1.0 mW, (B) 0.5 mW, and (C) 0.25 mW.

References

1. E. Hecht, *Optics*, 4th edn., Addison-Wesley, 2002.
2. P. Yeh, *Optical Waves in Layered Media*, Wiley, 2005.
3. K. Ohta and H. Ishida, *Appl. Opt.*, 1990, **29**, 1952-1959.
4. B. H. Ong, X. C. Yuan, S. C. Tjin, J. W. Zhang and H. M. Ng, *Sens. Actuator B-Chem.*, 2006, **114**, 1028-1034.
5. D. Axelrod, T. P. Burghardt and N. L. Thompson, *Annu. Rev. Biophys. Bioeng.*, 1984, **13**, 247-268.
6. D. Axelrod, in *Biophysical Tools for Biologists, Vol 2: In Vivo Techniques*, Elsevier Academic Press Inc, San Diego, 2008, vol. 89, pp. 169-221.
7. M. V. Klein and T. E. Furtak, *Optics*, John Wiley & Son Inc., New York, NY, 1986.

